

FIG.1

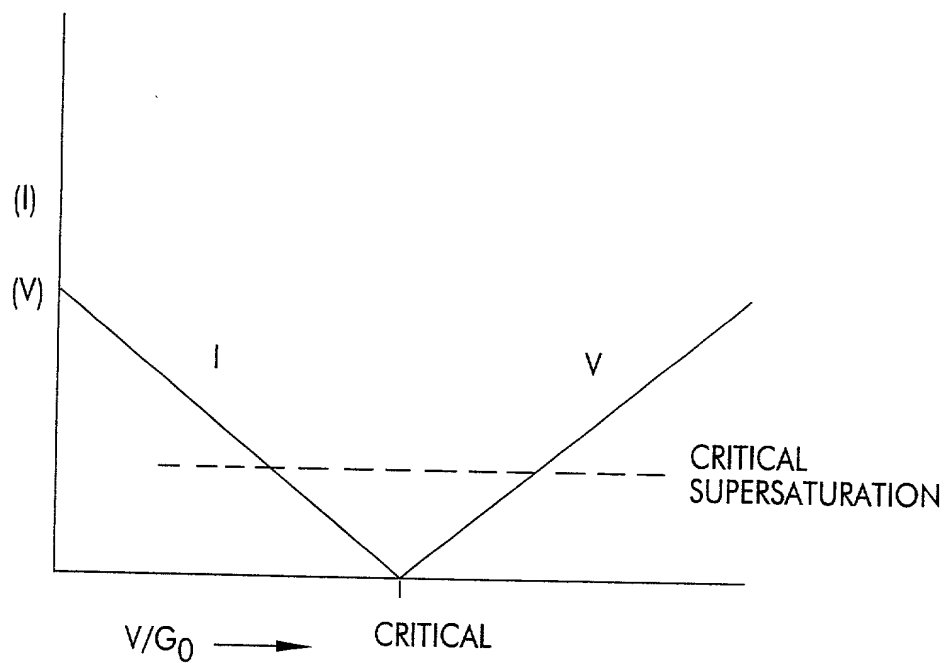


FIG.2

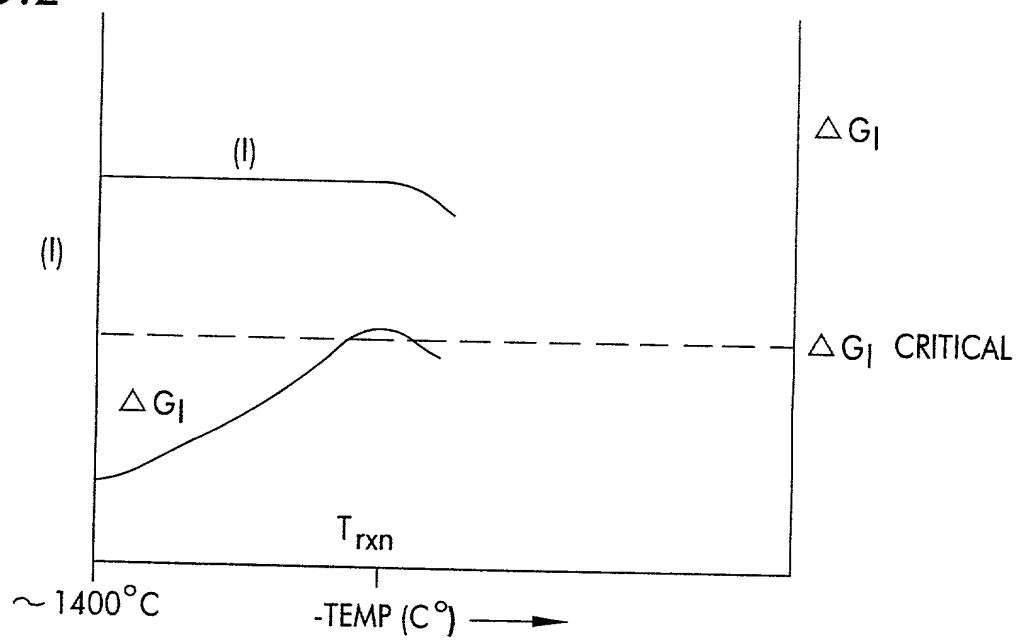


FIG.3

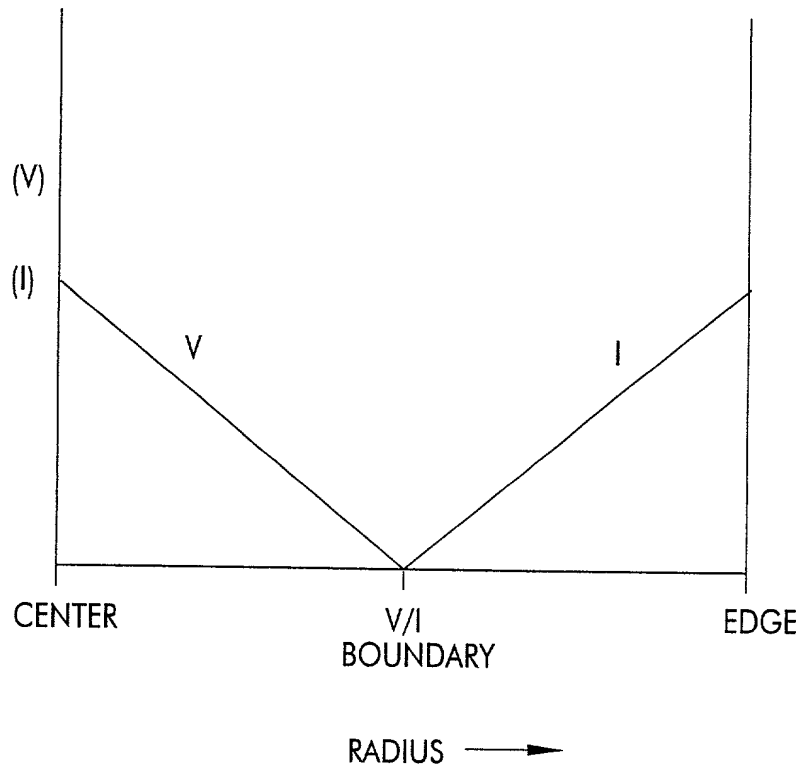


FIG.4

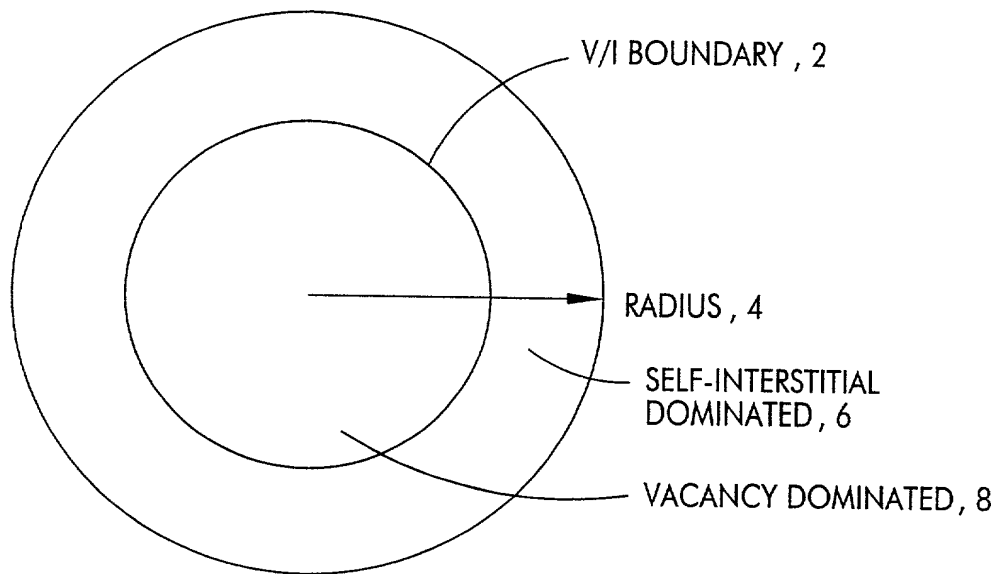


FIG.5

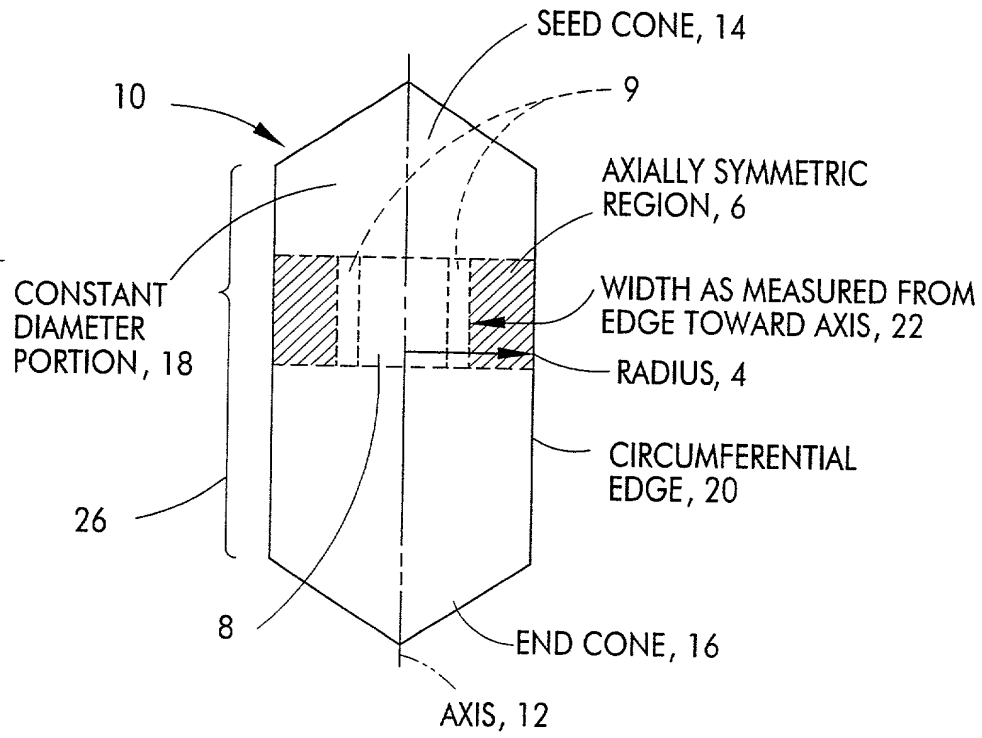


FIG. 6

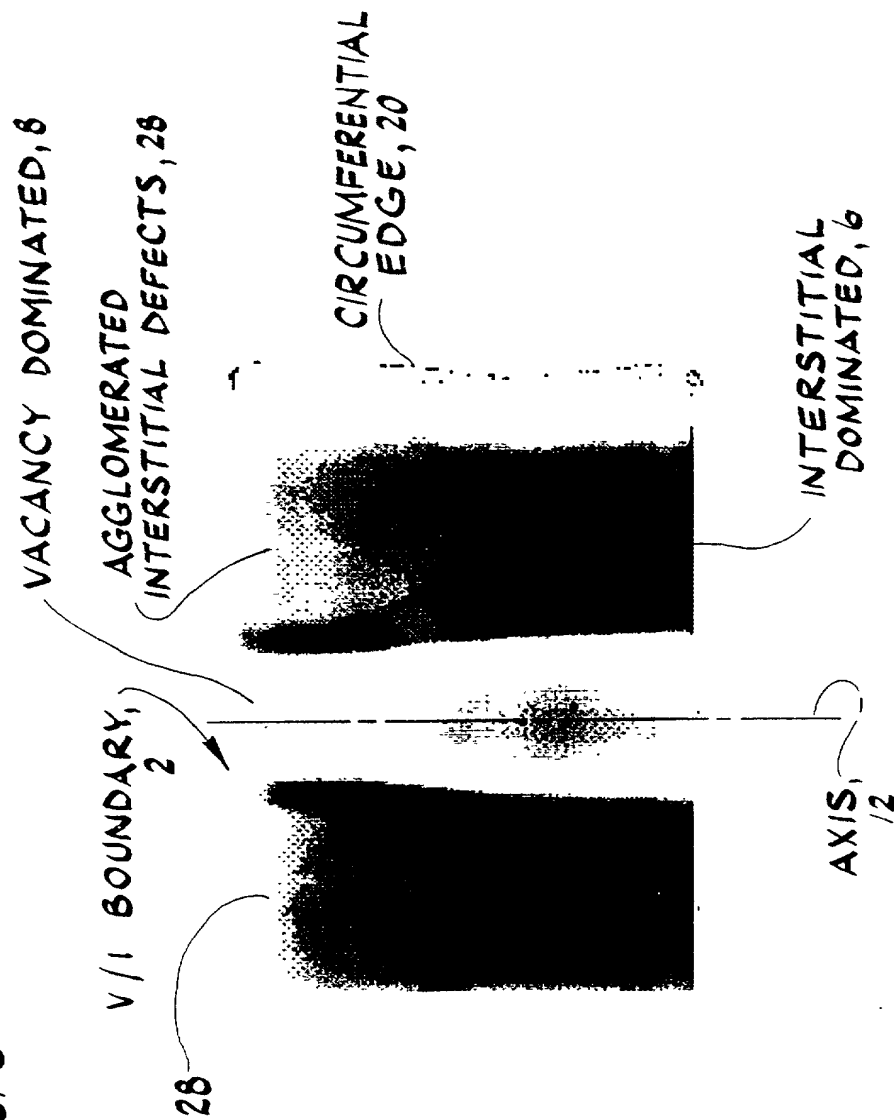
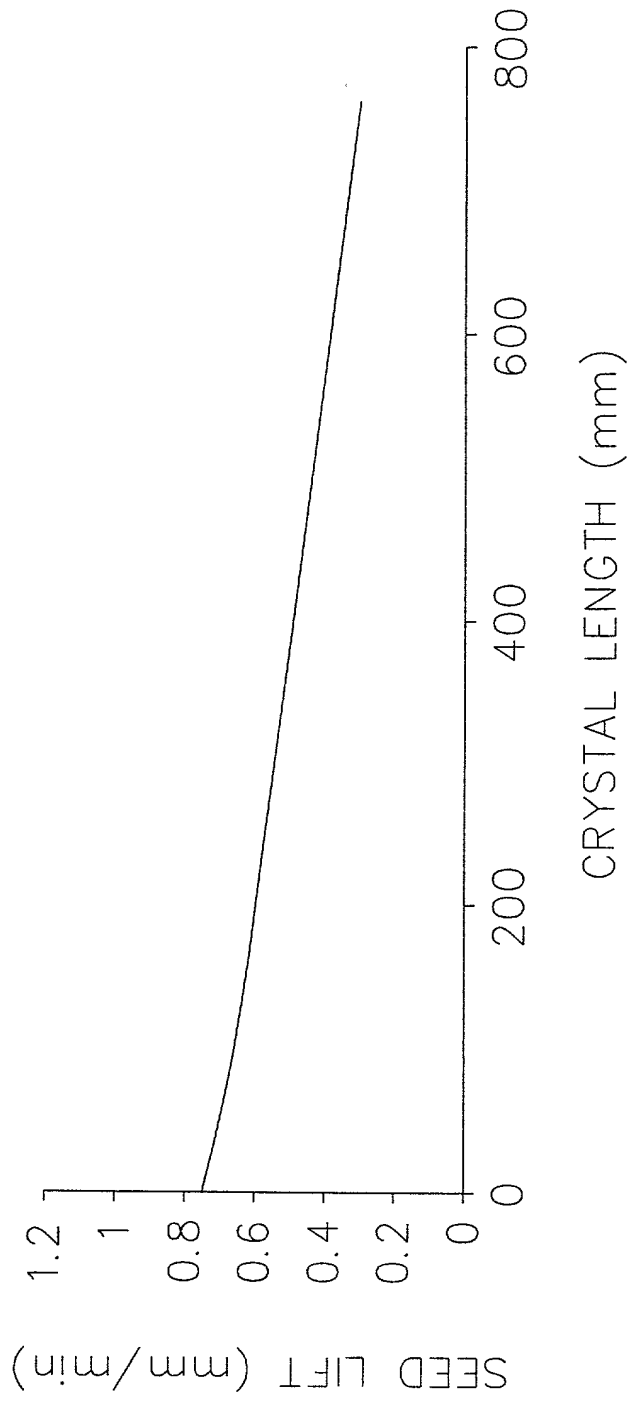


FIG. 7



001100-50382006

FIG. 8

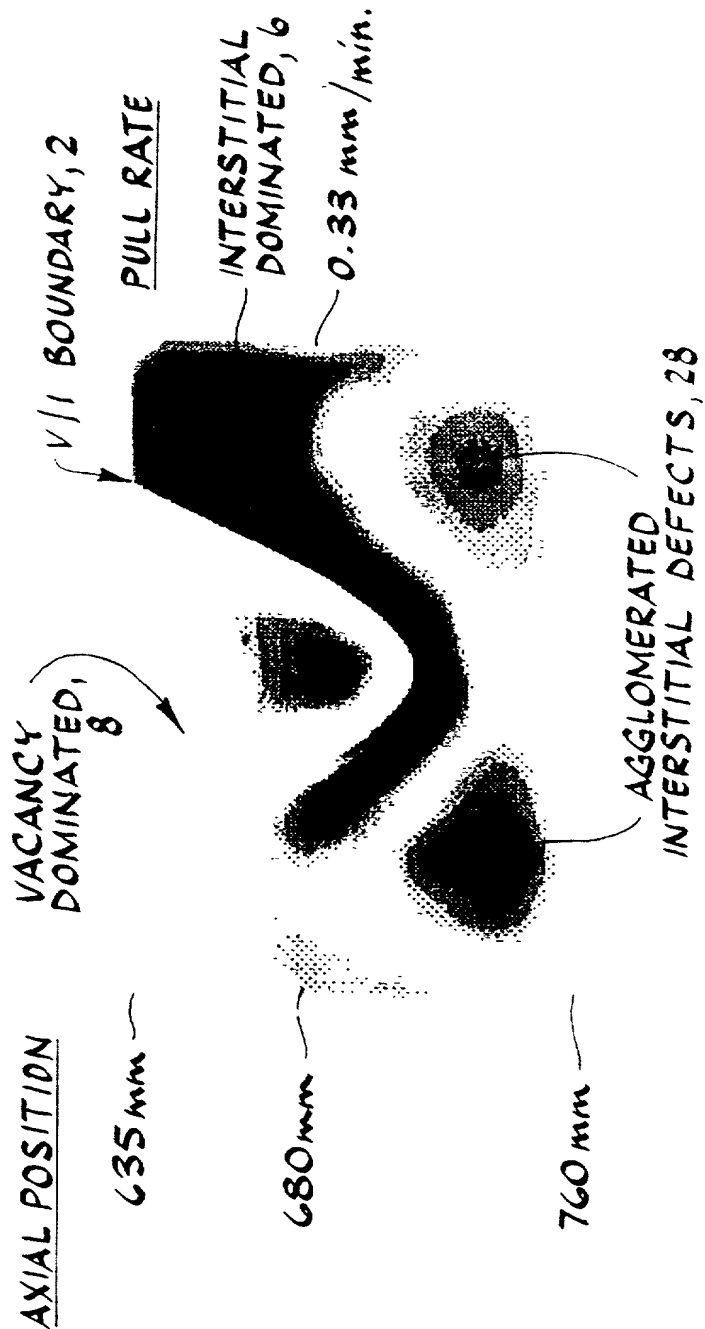


FIG. 9

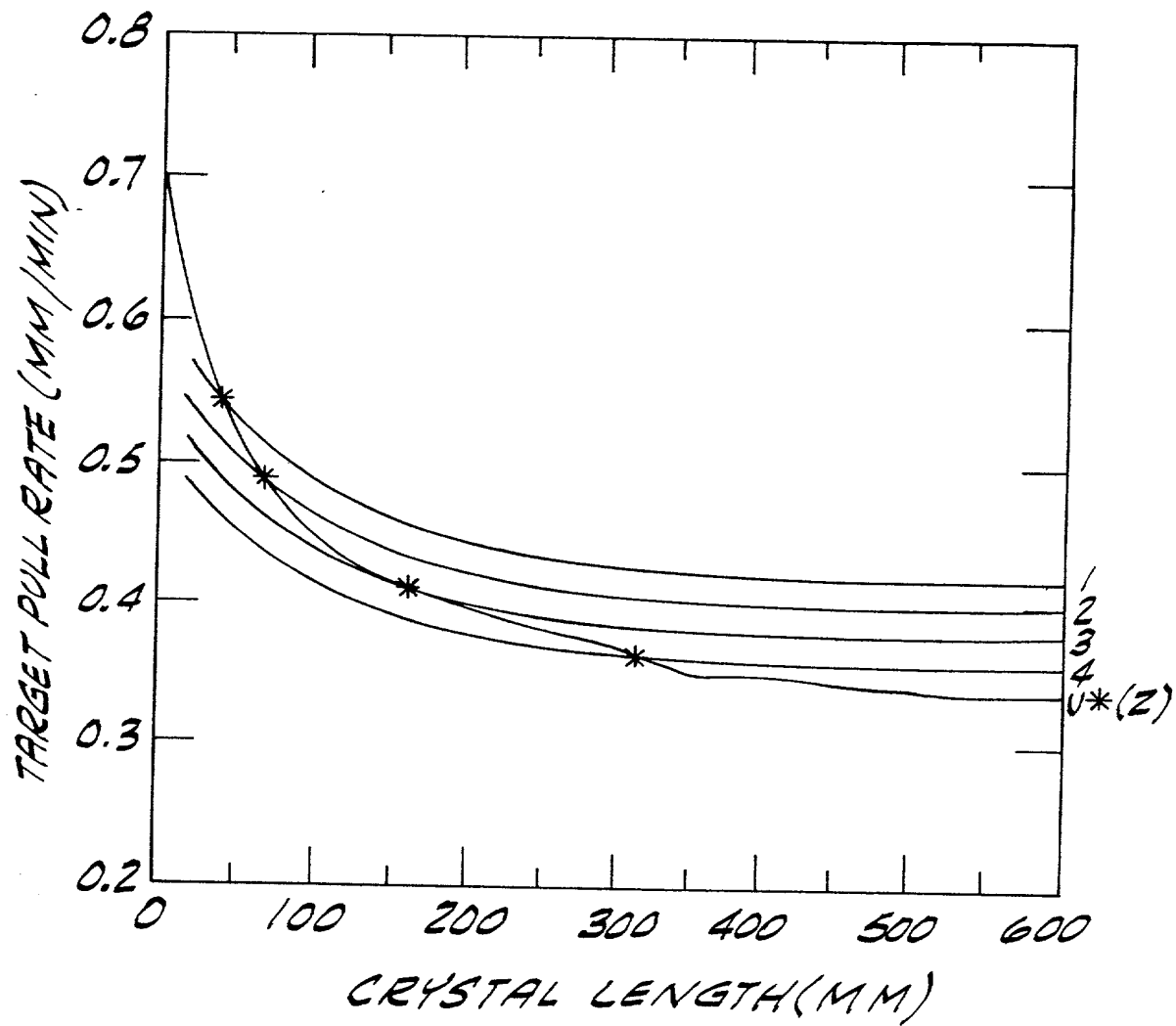


FIG. 10

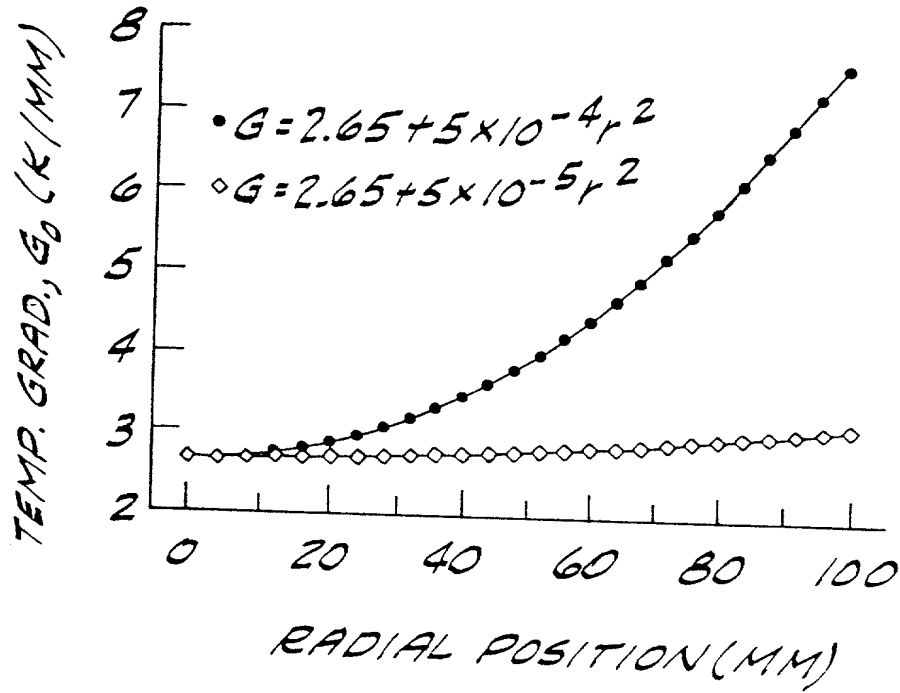


FIG. 11

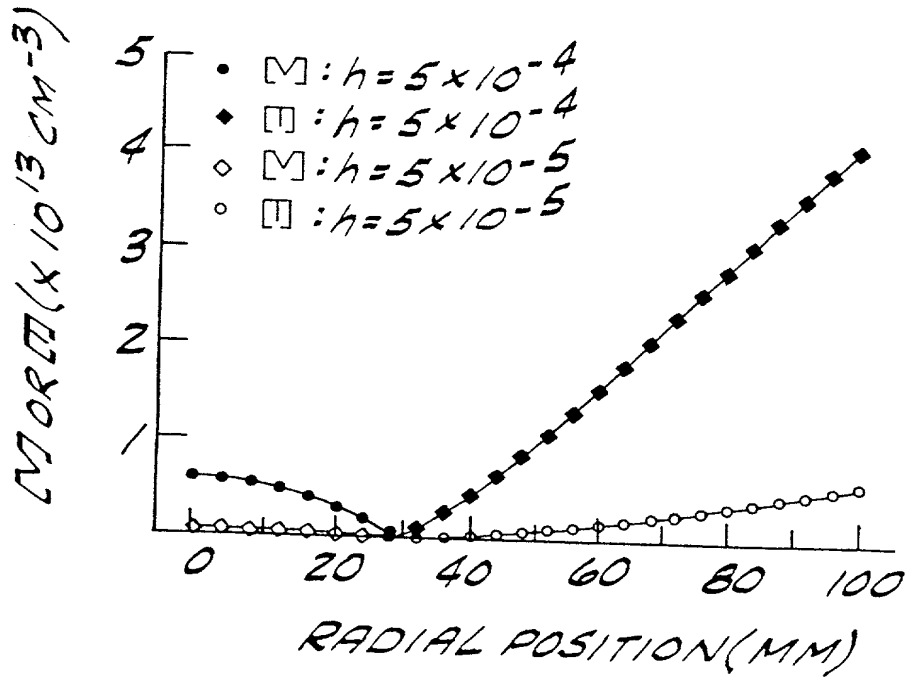




FIG. 12

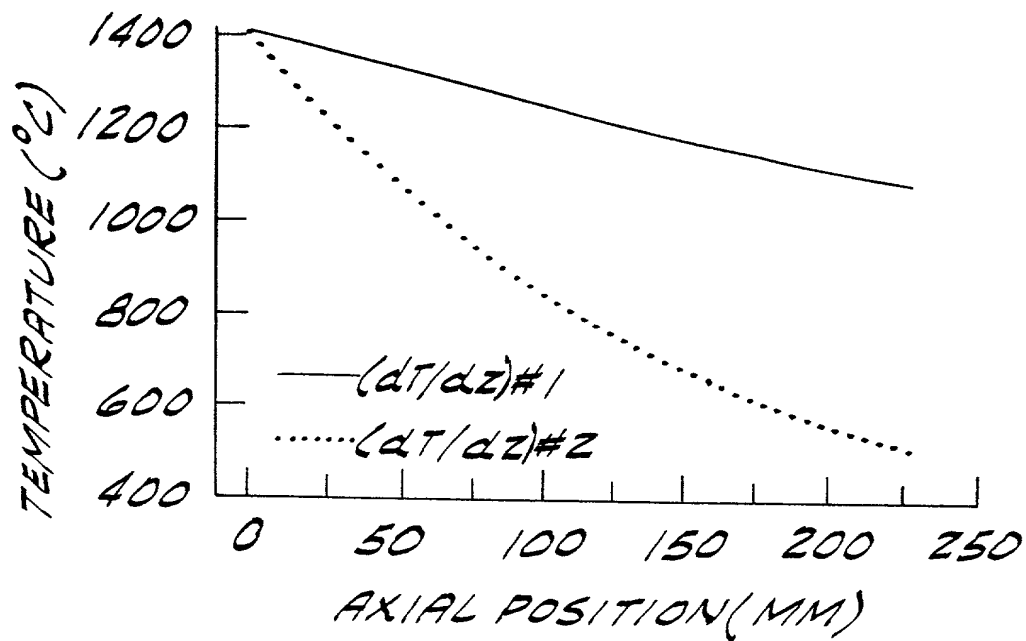
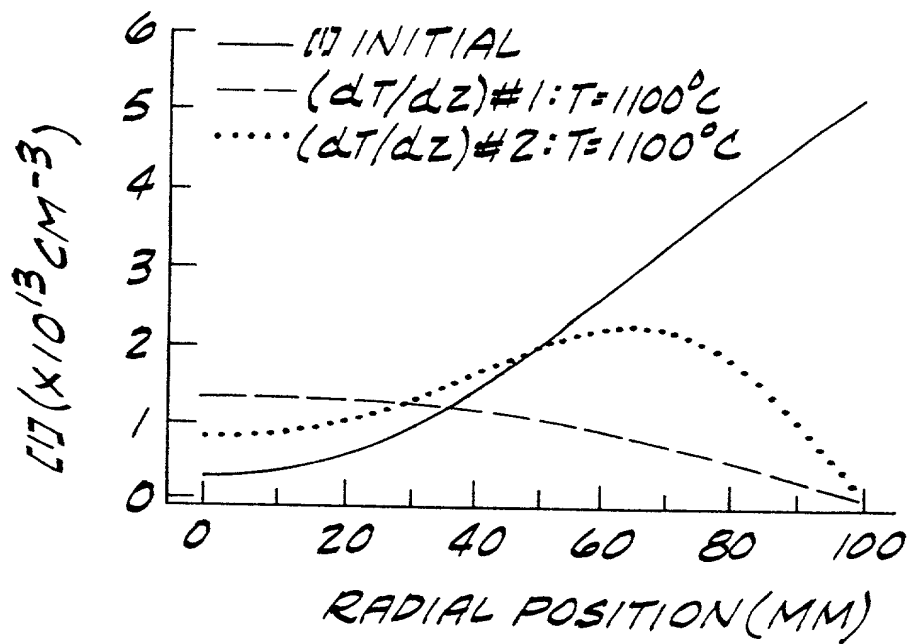


FIG. 13



201120-909E2001

FIG. 14

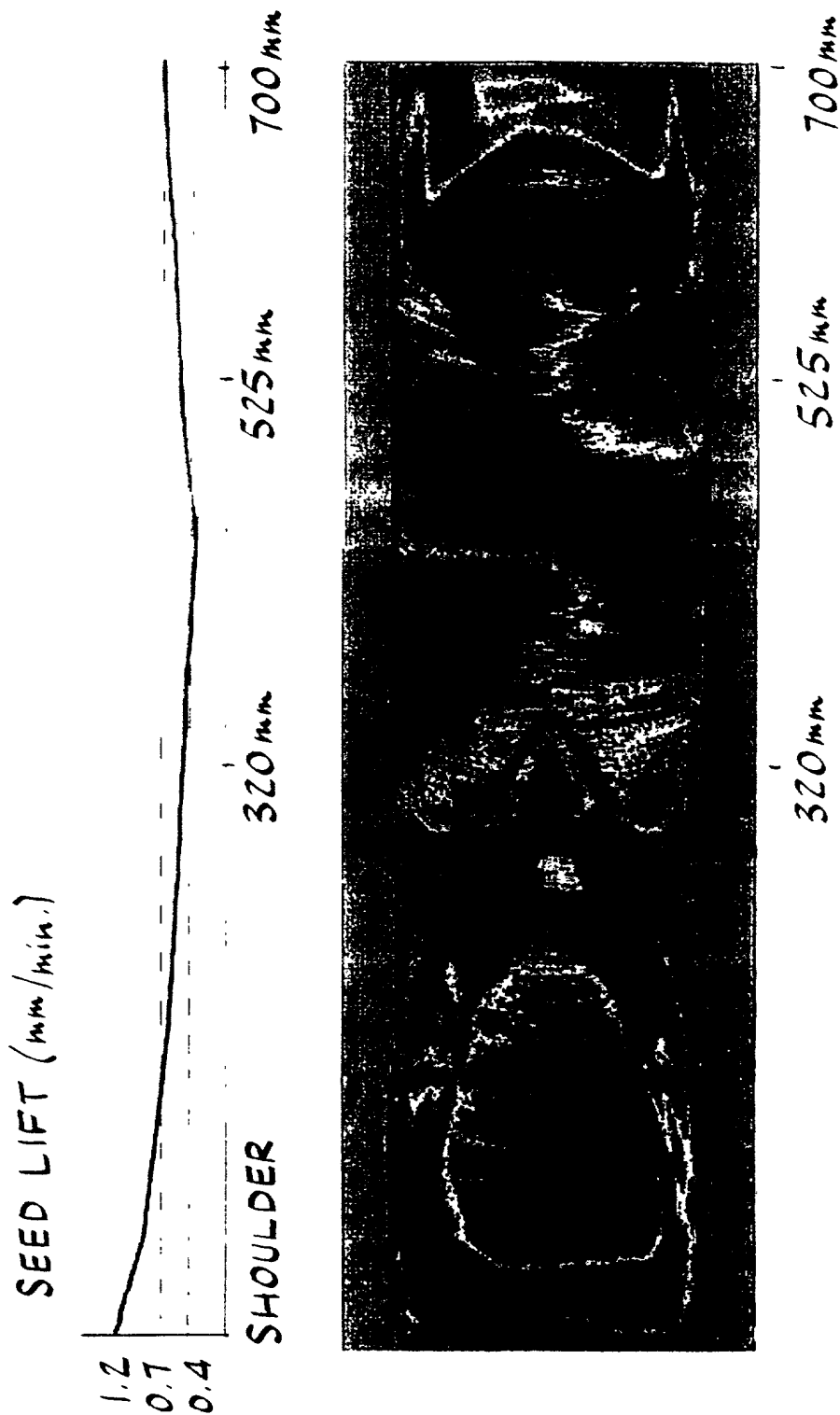


FIG. 15

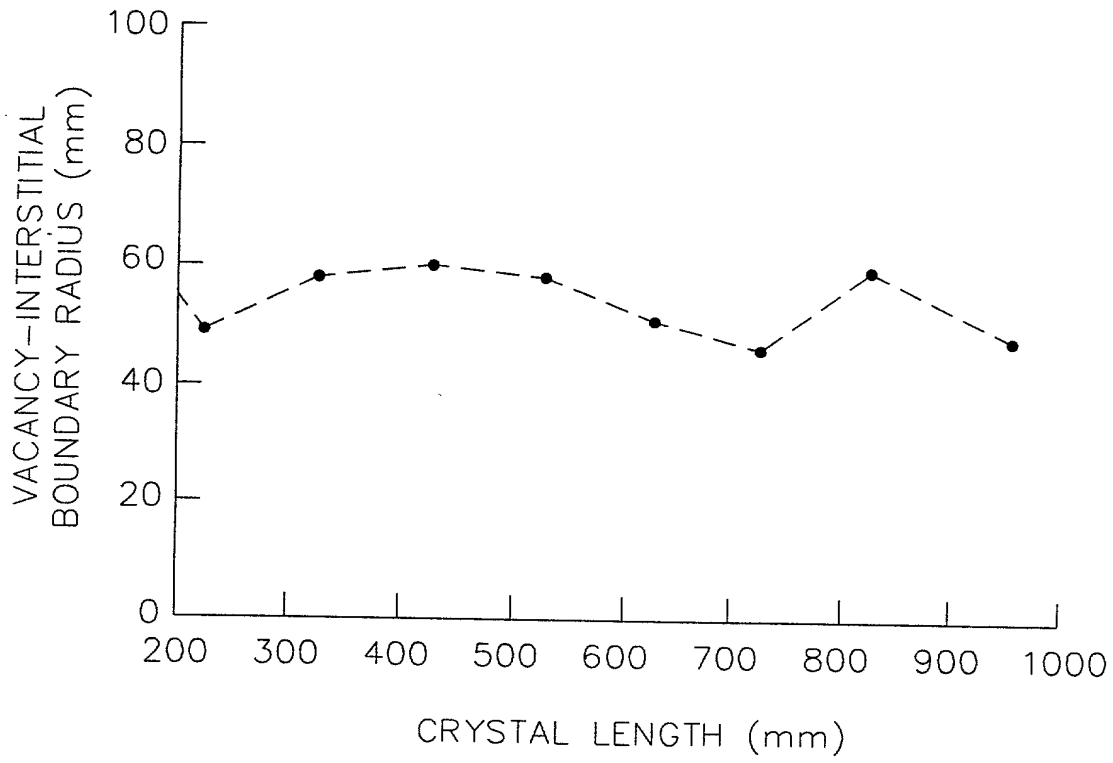


FIG. 16a

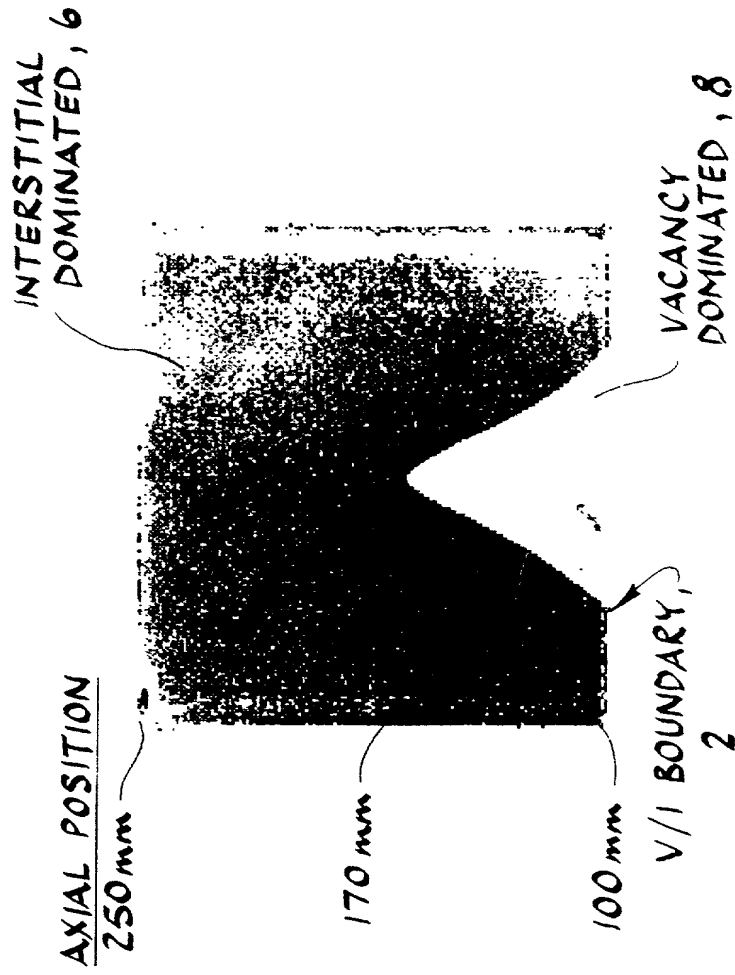




FIG.17

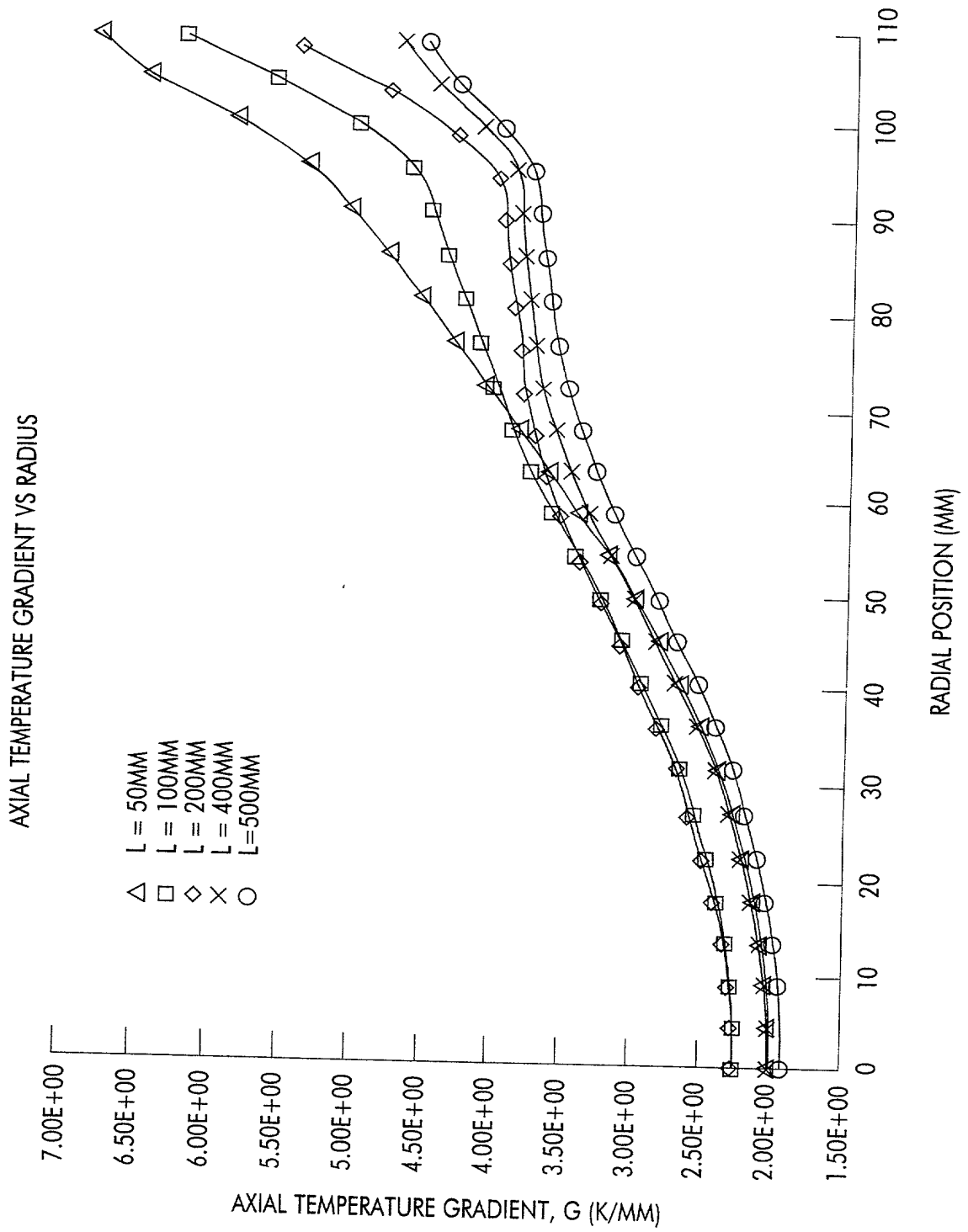
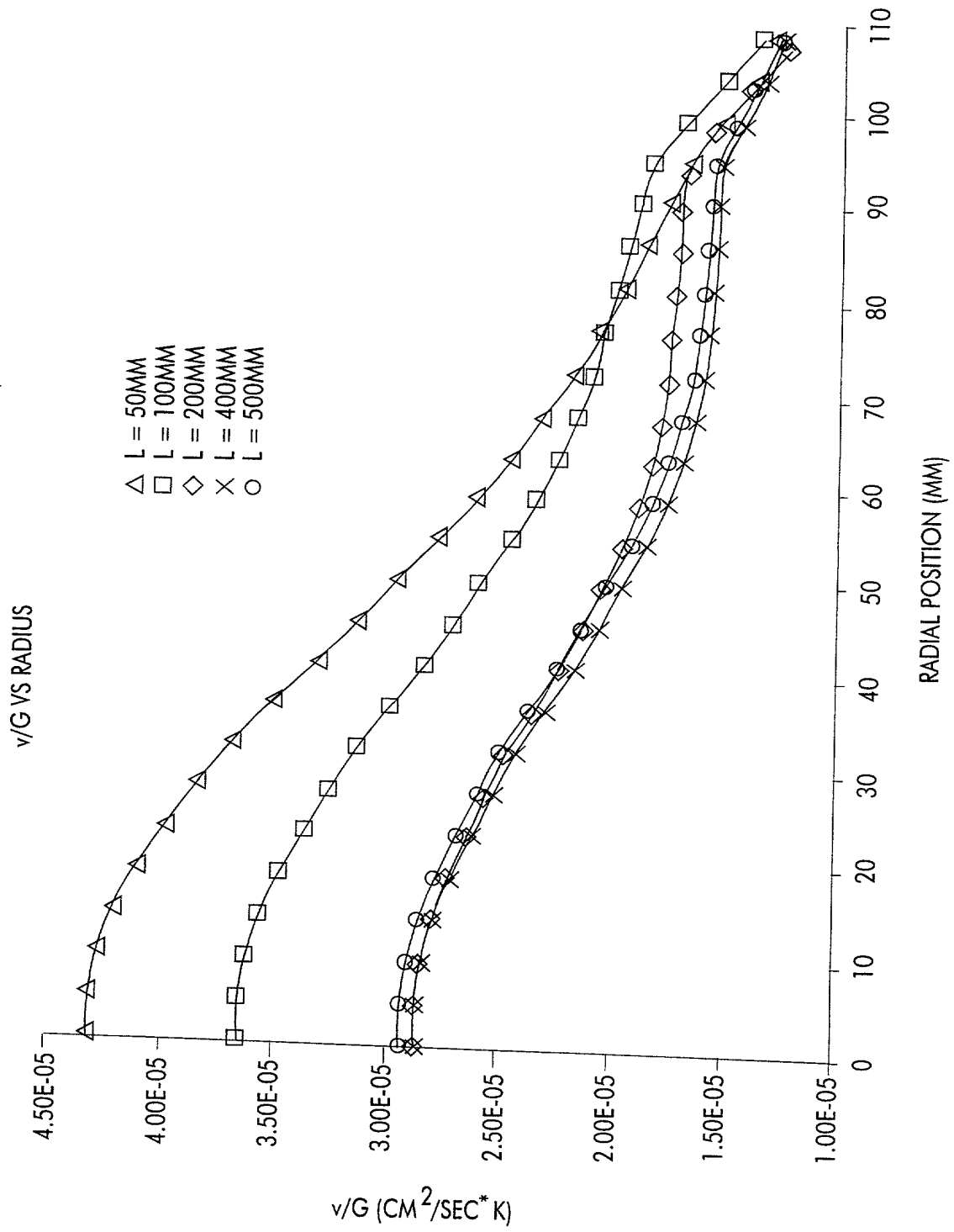


FIG.18



The graph plots the difference in crystal radius,  $R_{\text{CRYSTAL}} - R_{\text{VACANCY}}$  (in mm), against the cooling time to  $T = 1050^{\circ}\text{C}$  (in hours). The y-axis ranges from 0 to 110 mm, and the x-axis ranges from 0 to 40 hours. Two data series are shown: solid circles and open circles. The solid circles show a sharp increase in vacancy concentration starting around 11 hours, reaching a peak of approximately 105 mm at 15 hours, and then decreasing. The open circles show a similar trend, starting around 15 hours and reaching a peak of approximately 105 mm at 35 hours. A smooth curve is drawn through the solid circles, and a series of vertical lines connects the open circles to the x-axis.



FIG. 20

AXIAL  
POSITION

235 mm

255 mm

350 mm

V/I BOUNDARY, 2

VACANCY  
DOMINATED, 8

PULL RATE

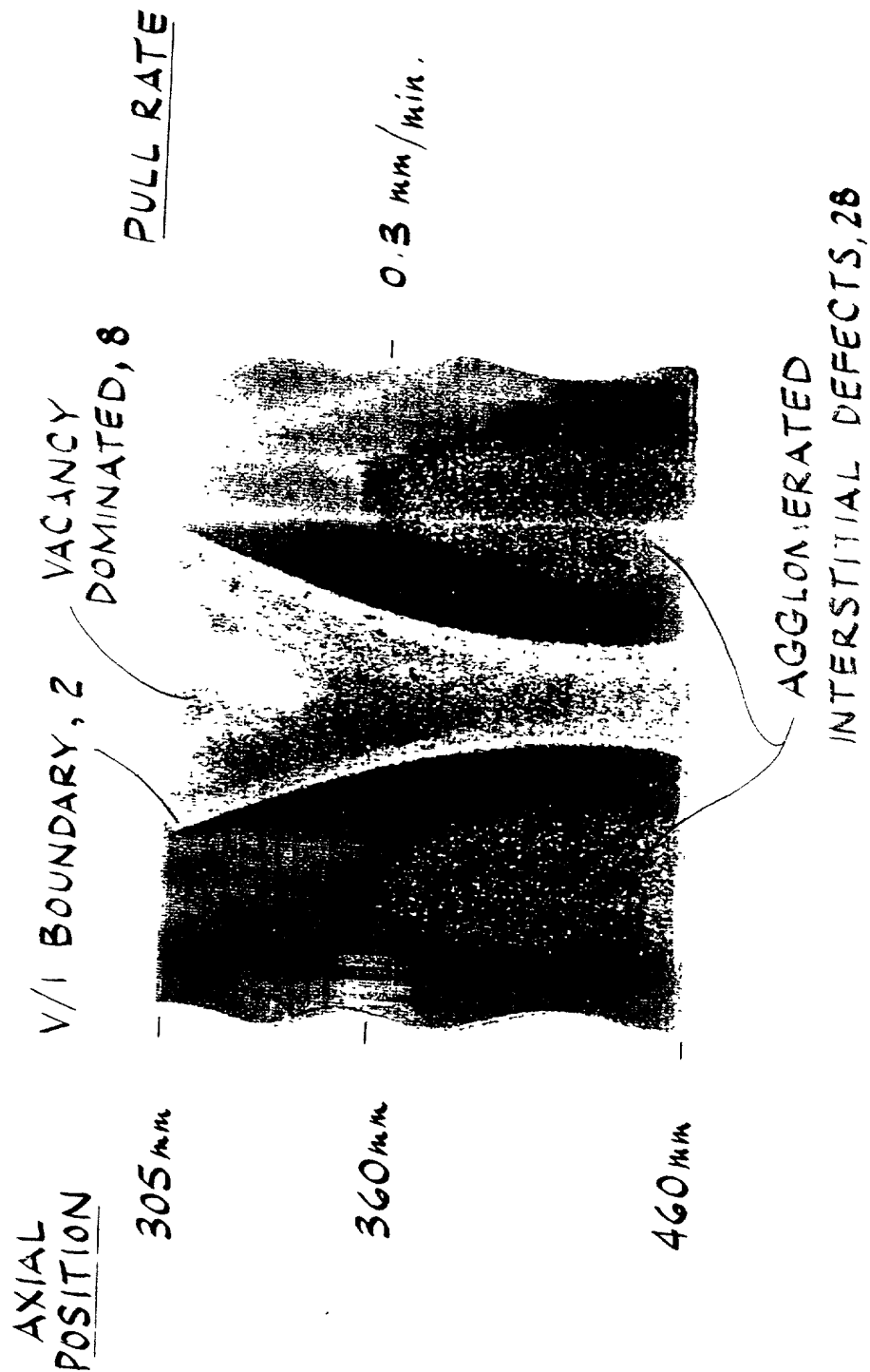
- 0.4 mm/min.



AGGLOMERATED  
INTERSTITIAL DEFECTS, 28

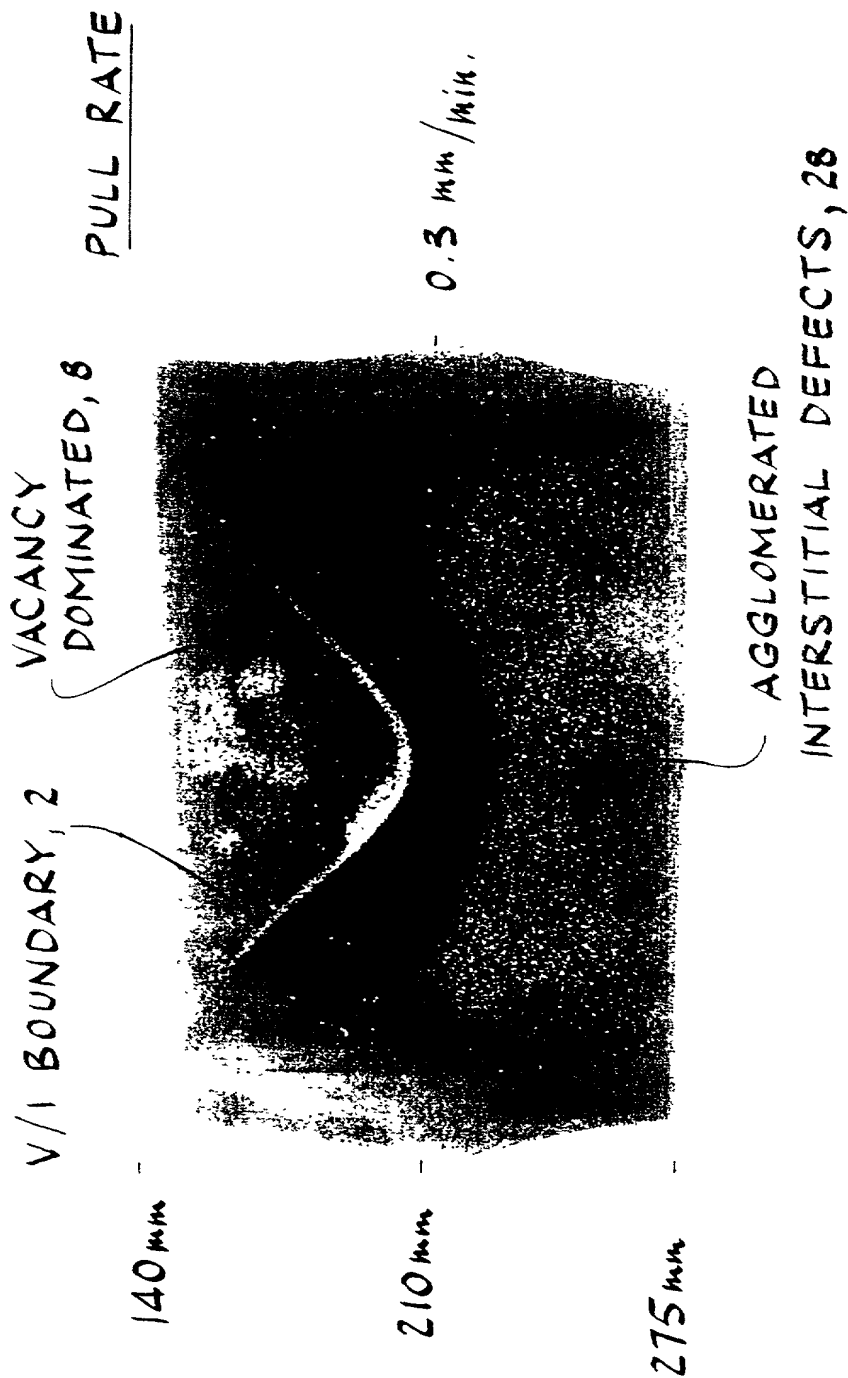
CONFIDENTIAL

FIG. 21



201420 90962001

FIG. 22



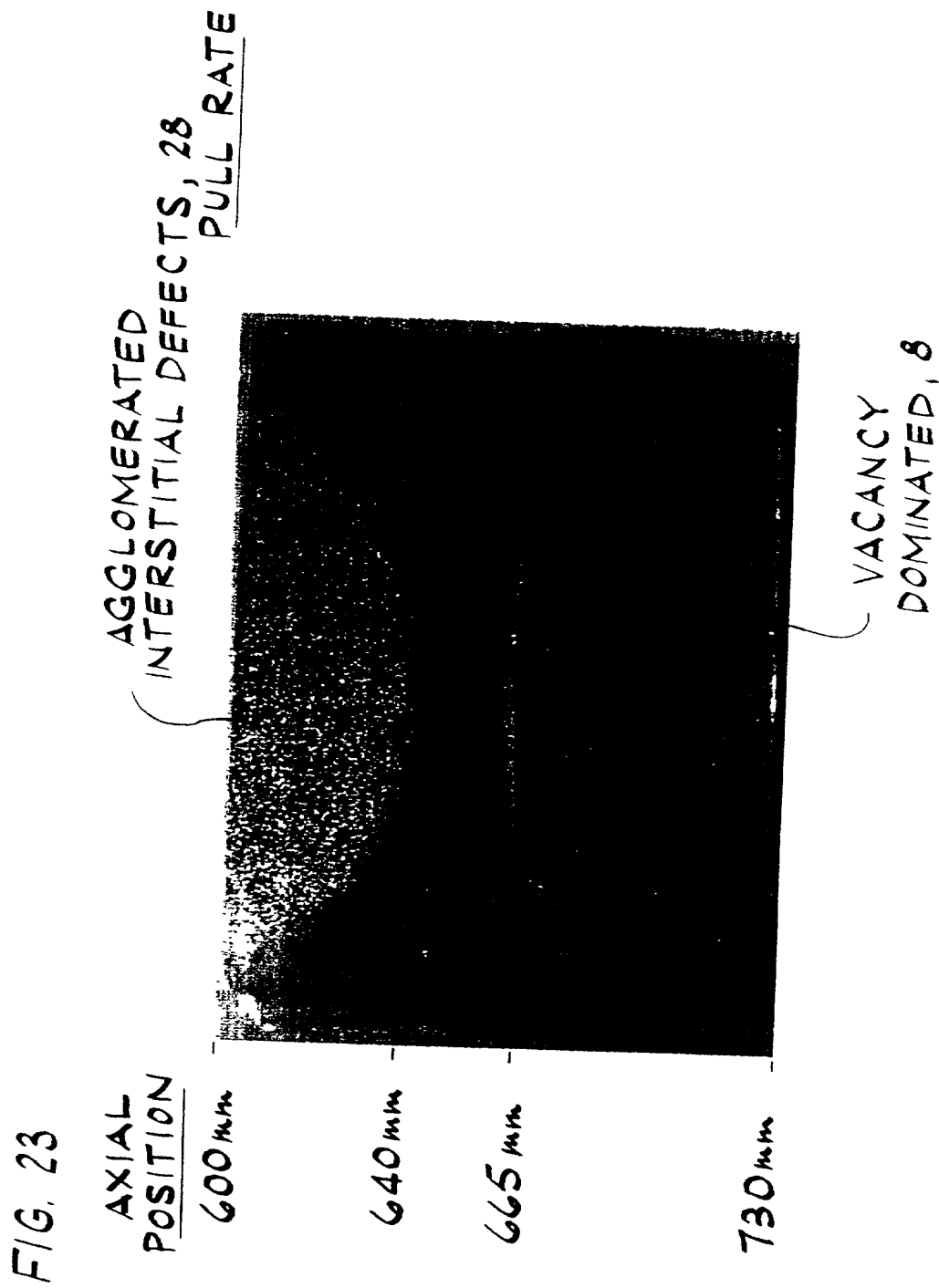


FIG.24

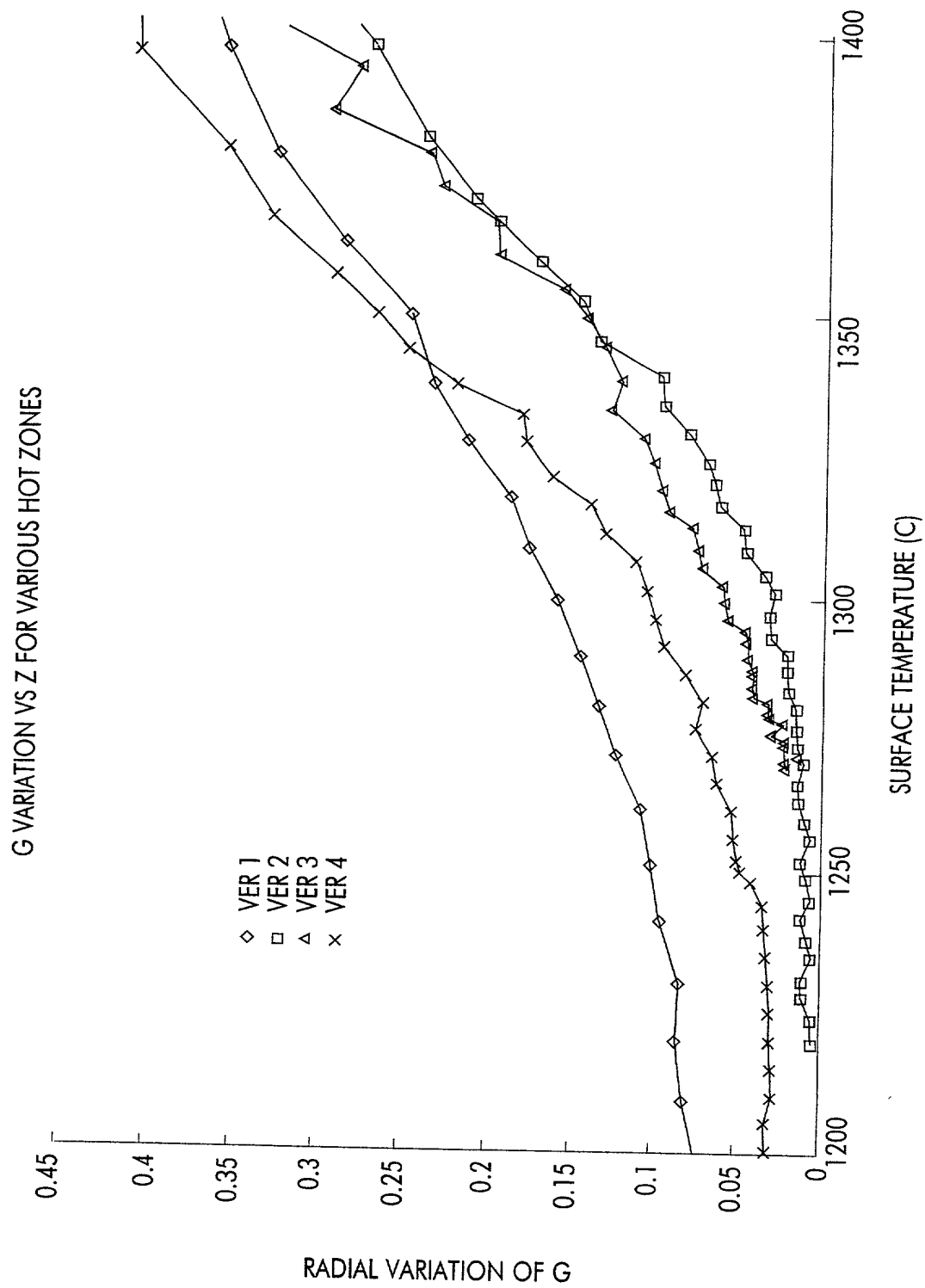


FIG.25

TEMPERATURE PROFILES FOR VARIOUS HOT ZONES

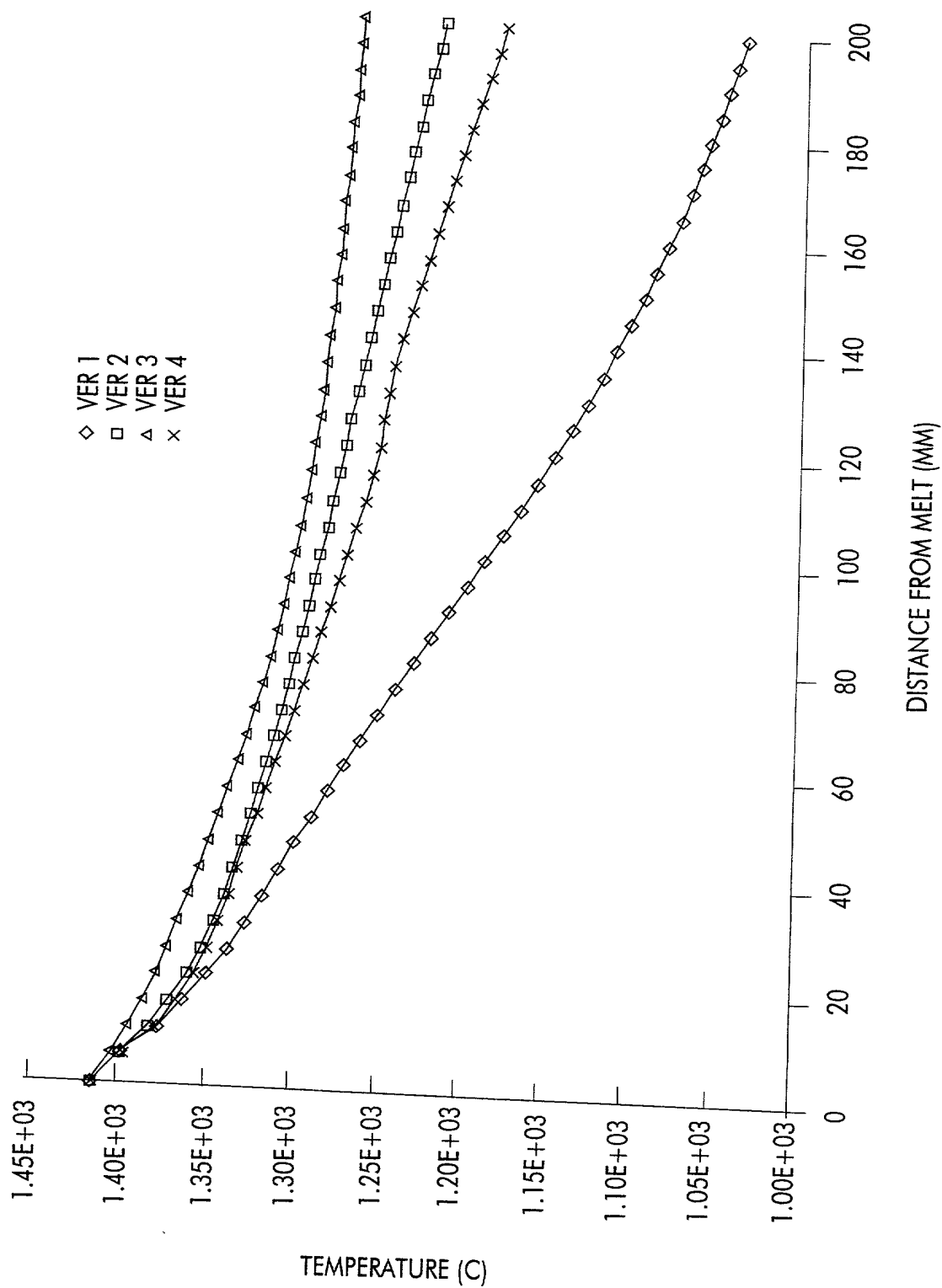


FIG. 26

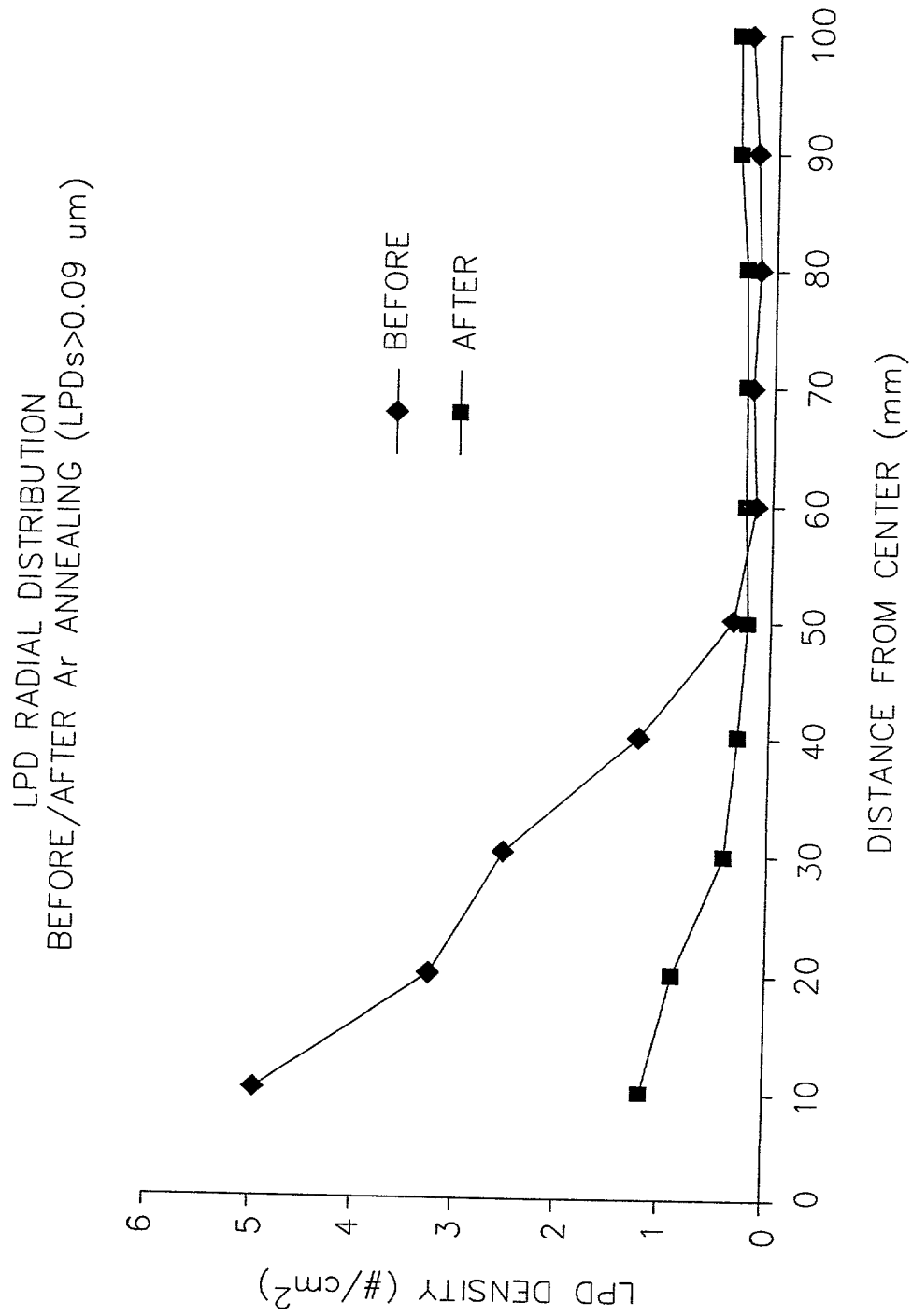


FIG. 27

LPD RADIAL DISTRIBUTION  
(BEFORE Ar ANNEALING: 0.09–0.11  $\mu\text{m}$ )

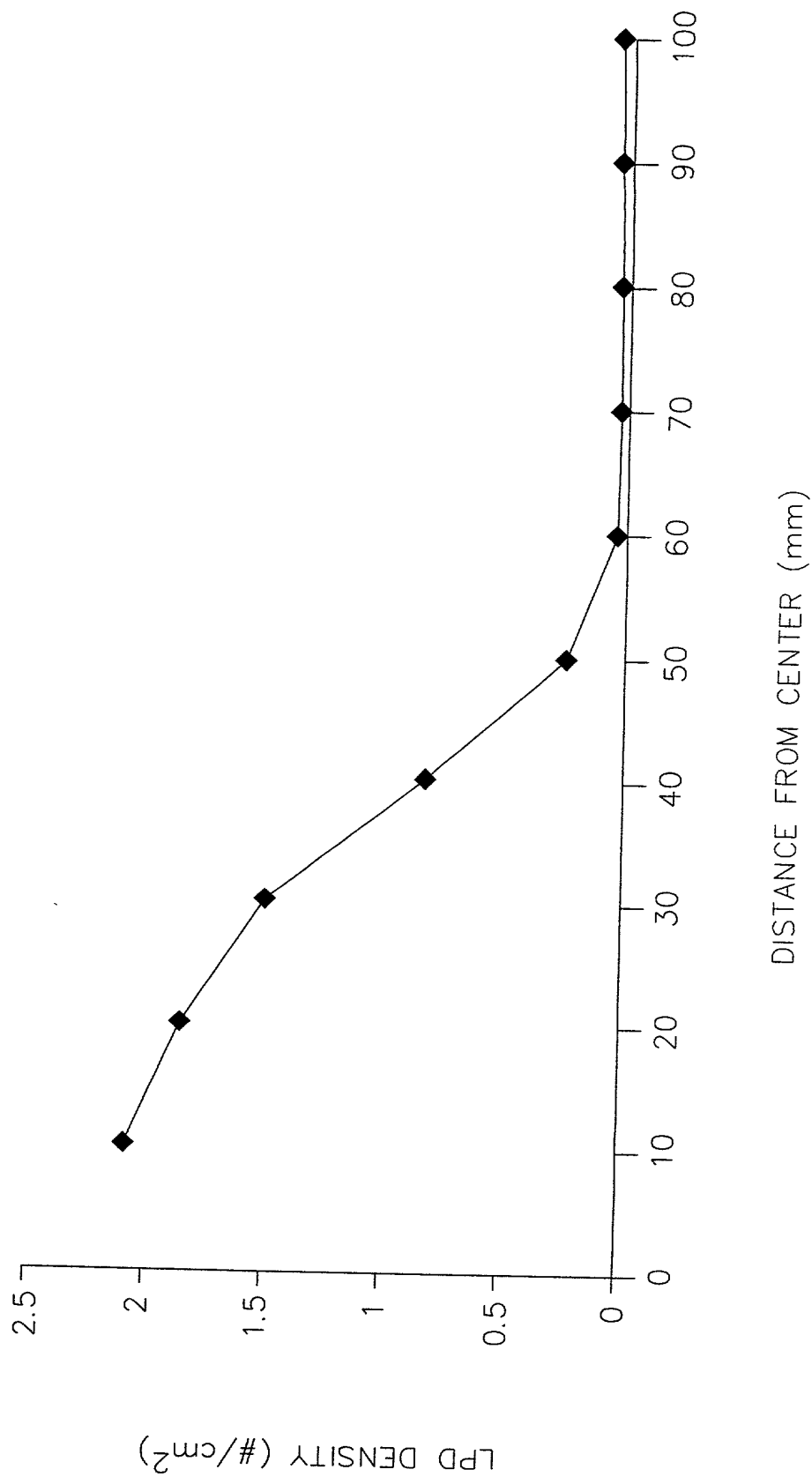




FIG. 28

LPD RADIAL DISTRIBUTION  
(AFTER Ar ANNEALING: 0.09–0.11  $\mu\text{m}$ )

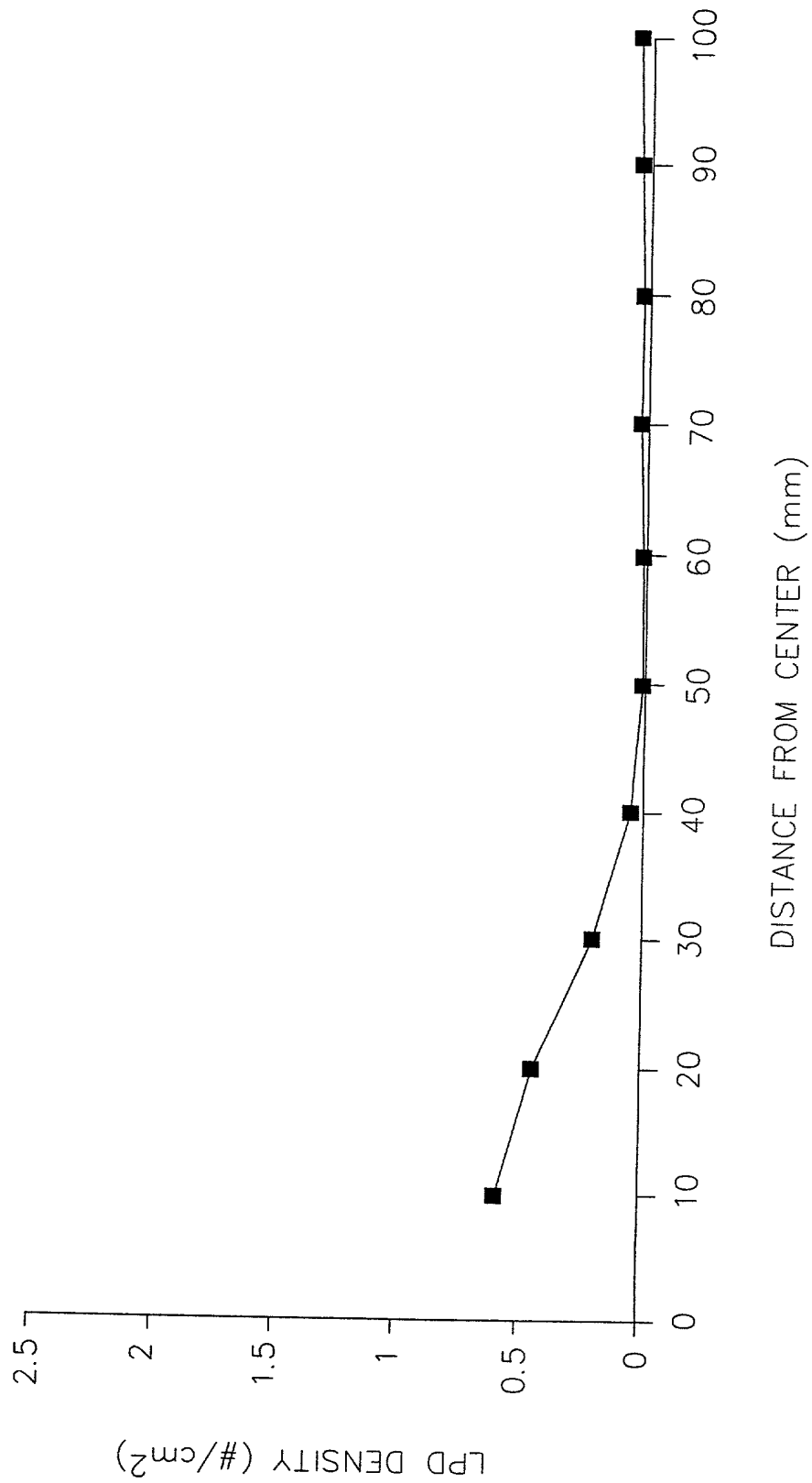


FIG. 29

LPD RADIAL DISTRIBUTION  
(BEFORE: 0.11-0.13  $\mu\text{m}$ )

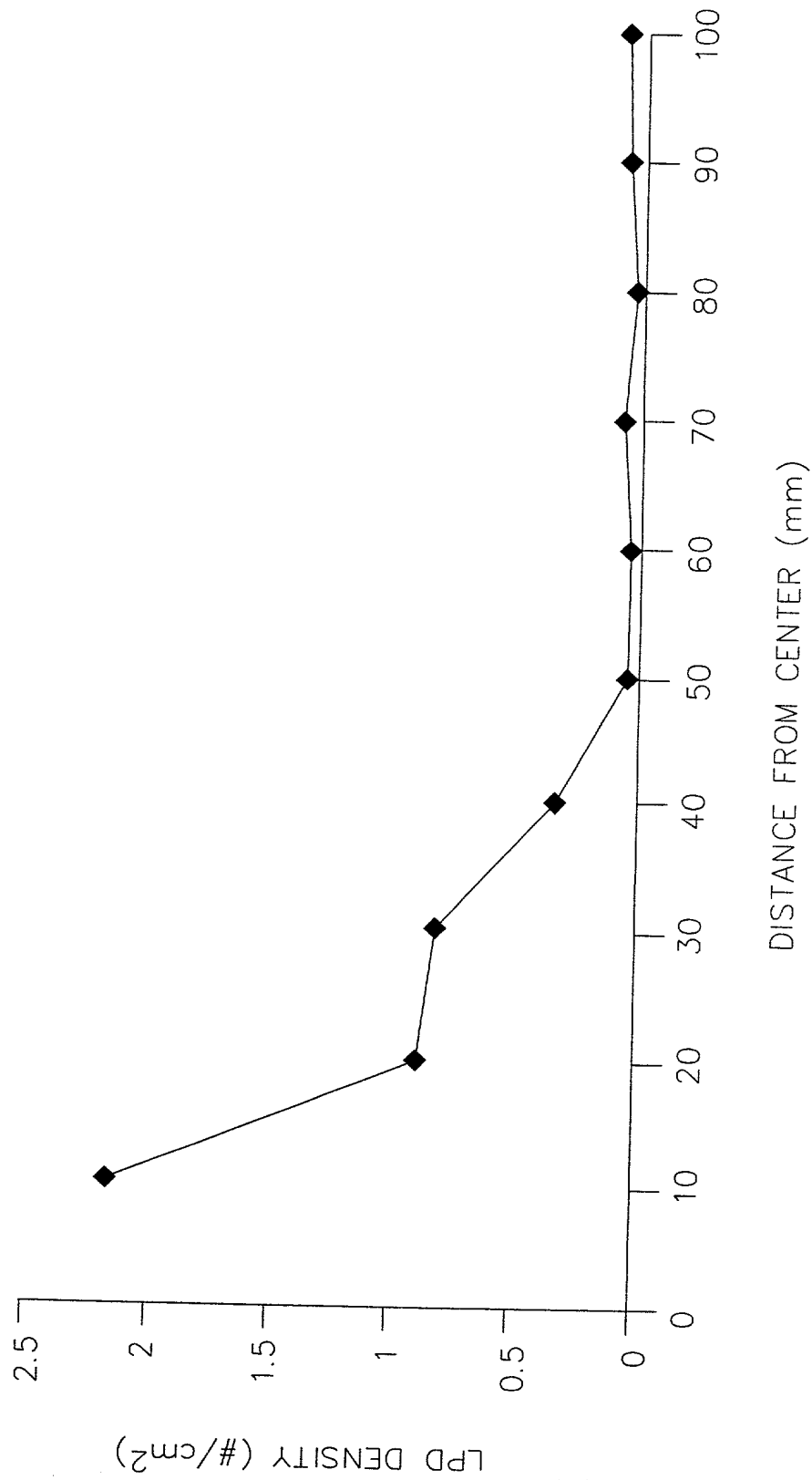


FIG. 30

LPD RADIAL DISTRIBUTION  
(AFTER Ar ANNEALING: 0.11-0.13  $\mu\text{m}$ )

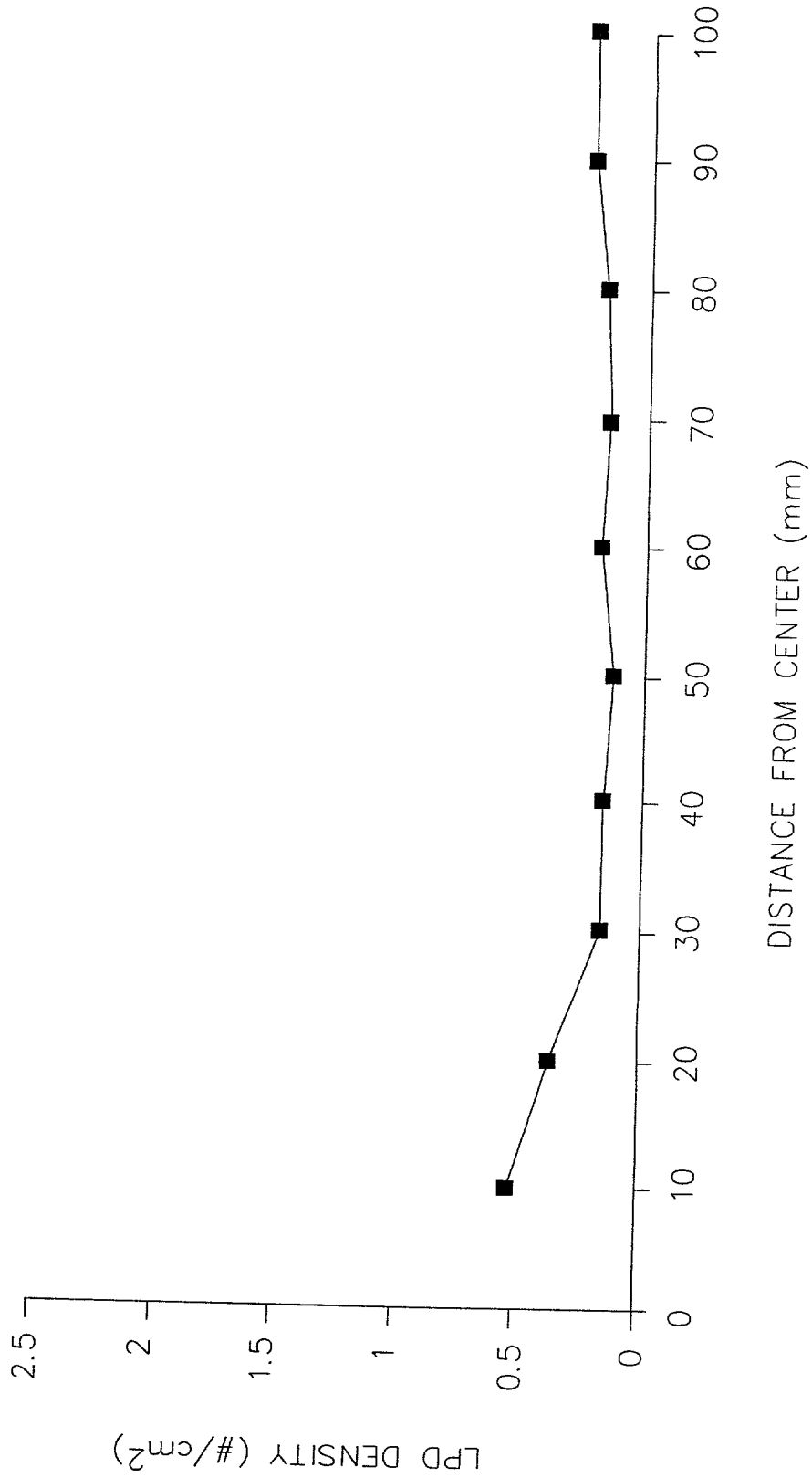


FIG. 31

LPD RADIAL DISTRIBUTION  
(BEFORE: 0.13-0.15  $\mu\text{m}$ )

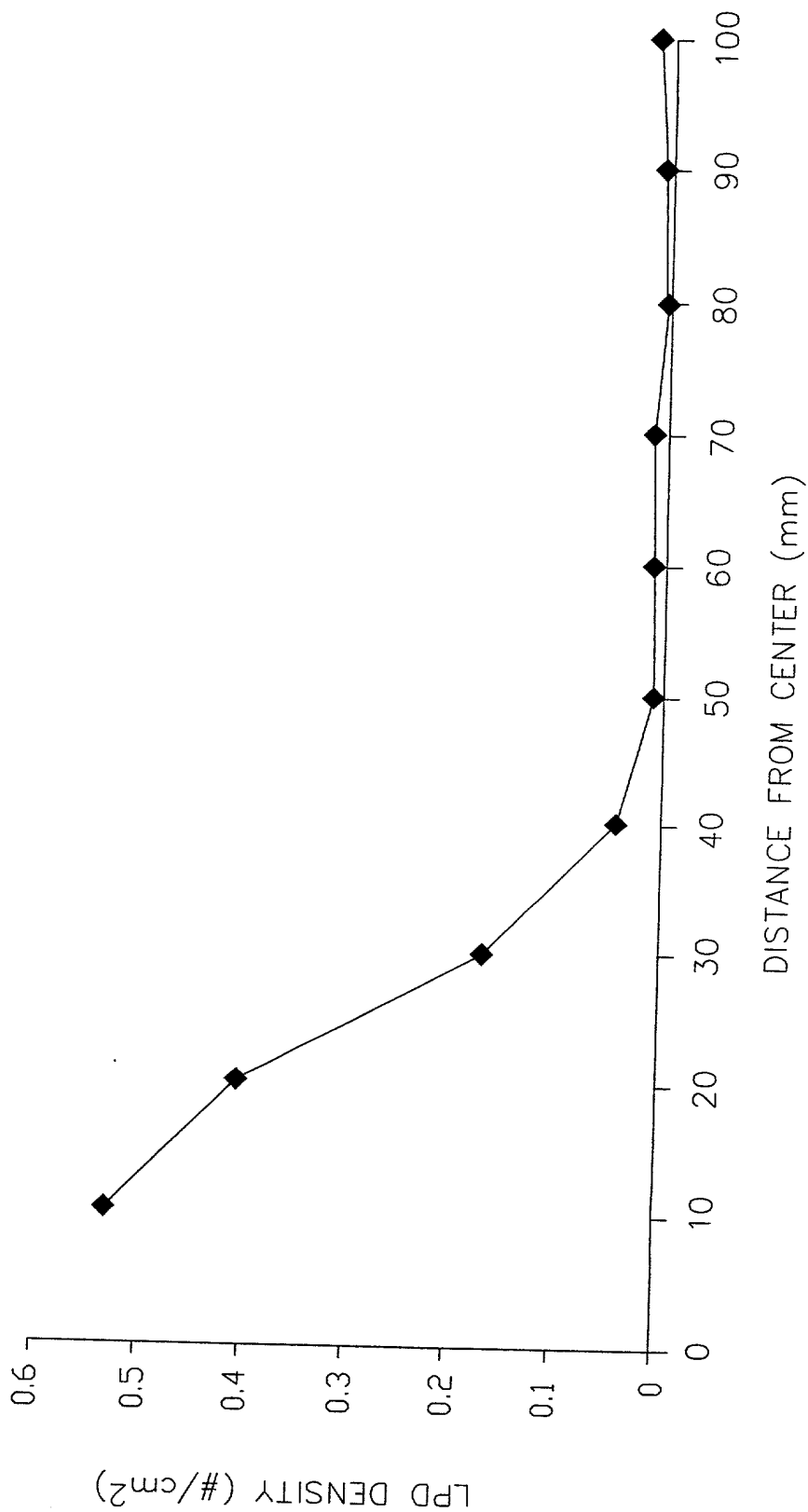


FIG. 32

LPD RADIAL DISTRIBUTION  
(AFTER Ar ANNEALING: 0.13-0.15  $\mu\text{m}$ )

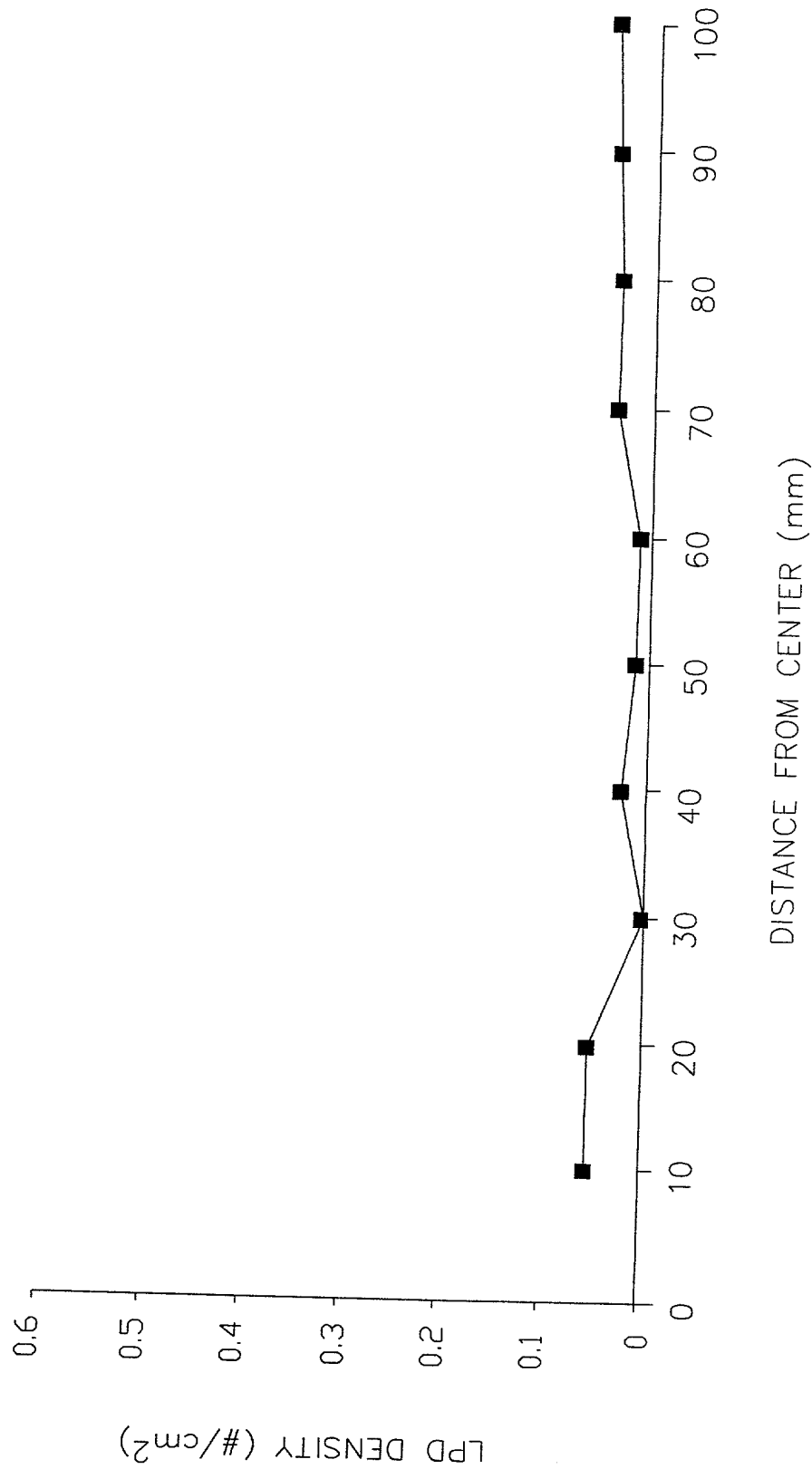


FIG. 33a

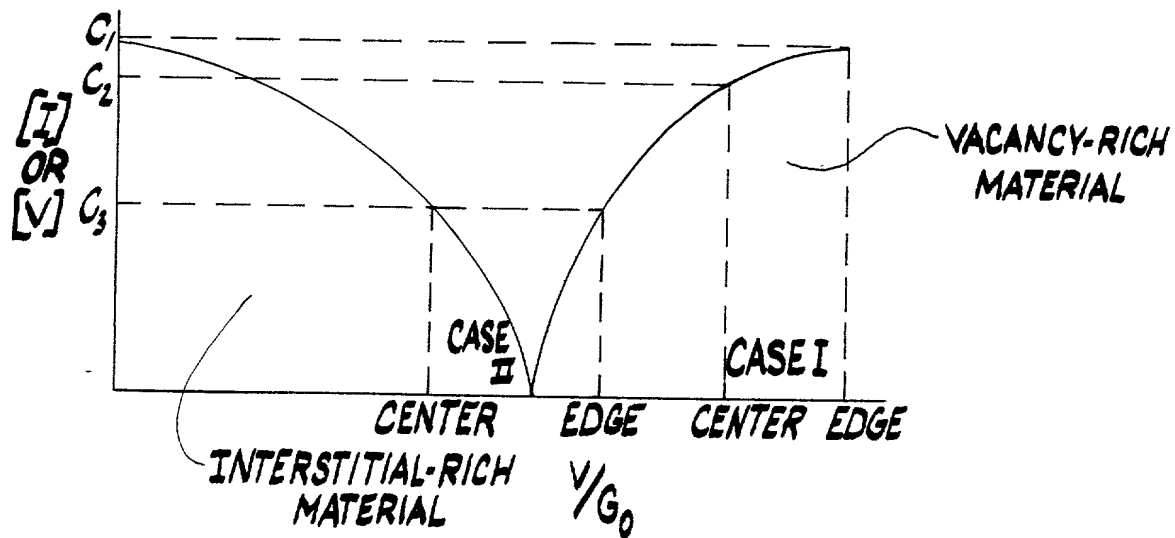


FIG. 33b

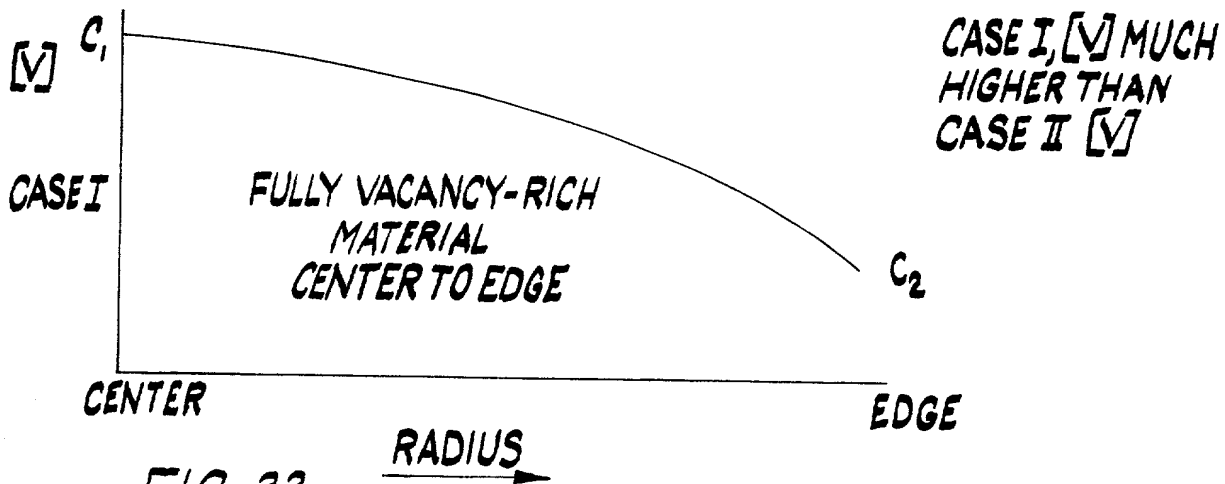


FIG. 33c

